

Role of the Succinate Skeleton in the Disorder–Order Transition of AOT and Its Analogous Molecules: Detection by Infrared Absorption Spectra of the Configurations Arising from the Difference in Torsion Angles of the Succinate Skeleton

Hiro-Fumi Okabayashi,*[1] Ken-Ichi Izawa,[2] Akiko Sumiya,[1] Julian Eastoe,[3] and Charmian J. O'Connor[4]

[1]Department of Applied Chemistry, Nagoya Institute of Technology, Gokiso-cho, Showa-ku, Nagoya 466-8555

[2]Technical Center, Fuji Silysia Chemical Ltd., 16303-3 Aza-Kihara, Oaza-Hichiya, Hyuga 883-0062

[3]School of Chemistry, University of Bristol, Cantock's Close, Bristol, BS81TS, U.K.

[4]Department of Chemistry, The University of Auckland, Private Bag 92019, Auckland 1142, New Zealand

Received January 5, 2010; E-mail: fwiw4348@mb.infoweb.ne.jp

The IR spectra in the 1300–1450 cm^{-1} region, which reflect the CH and CH_2 deformation vibrational modes of the succinate skeleton, have been investigated in detail for sodium dialkylsulfonates (alkyl groups: ethyl, *n*-propyl, *n*-butyl, *n*-hexyl, *n*-heptyl, *n*-octyl, *n*-decyl, and *n*-dodecyl) and sodium 1,2-bis(2-ethylhexyl)sulfosuccinate (sodium 1,2-bis(2-ethylhexyloxycarbonyl)ethanesulfonate) (AOT). The results have provided clear evidence that two configurations, arising from the difference in the torsion angles of the succinate skeleton, are preferentially stabilized in aqueous solution as well as in the solid state, depending upon the concentration. Thus, the IR spectra of this region can be used as a powerful tool for elucidation of the mechanism of the disorder–order transition in aggregate systems of AOT or its homologs at the molecular level.

Extensive studies have been made in elucidation of the physical properties of normal and reversed micelles formed by various surfactant molecules. In particular, vibrational spectroscopic methods have been recognized as powerful tools for investigating the microstructures of such aggregate systems.[1–19]

The Raman scattering spectra of simple surfactant molecules[1–3,6,7] have provided direct evidence that, of all the possible rotational isomers about the CH_2–CH_2 (or CH_2–CH=) single bond, one specific isomer (all-*trans* form for *n*-alkyl chains) is preferentially stabilized upon aggregation in water. These results indicate that the conformational transition of surfactant molecules is always attended by the disorder–order transition and that a hydrophobic interaction is the only driving force for such a conformational transition.

Furthermore, we have demonstrated that *N*-acylglycine oligomers[18,19] form their aggregates by stabilizing a specific isomer, in which formation of hydrogen bonds, as well as a hydrophobic interaction, are critical to stabilization.

The concept that the conformational transition of surfactant molecules occurring upon aggregation may be critical to investigation of the mechanism of the shape variation of an aggregate. Such a conformational change varies the so-called packing parameter, P_p, of a surfactant molecule, according to the equation $P_p = v_s/(a_H l_C)$, where v_s, a_H, and l_C are effective molecular volume, effective water contact area per molecule, and effective molecular length, respectively.[20] Accordingly, use of this packing parameter to explain the shape-transition of an aggregate requires elucidation of the conformational transition of the surfactant molecule.

The molecules of AOT and its analogs have a succinate skeleton (–$^{2'}$C(=O)–$^{1'}$C–^{1}C–^{2}C(=O)–) in common (Scheme 1), in addition to the two hydrocarbon chains, which result in such a conformational transition upon aggregation. Some rotational isomers are possible for the succinate skeleton, and out of all the rotational isomers, stabilization of one specific isomer

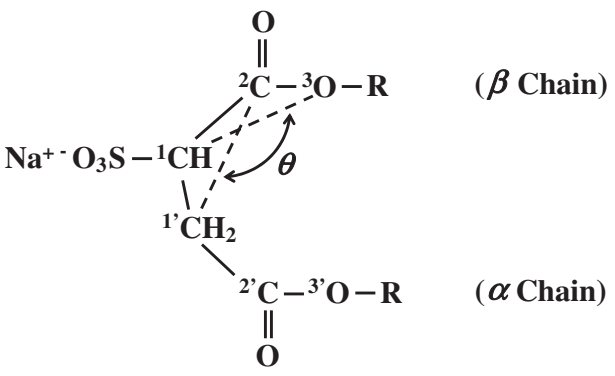

R: 2-ethylhexyl chain for AOT and *n*-alkyl chains for AOT-homologues

Scheme 1. Atomic numbering of the molecular formula of the succinate segment of AOT and its homologs. θ denotes the torsion angle of the $^{1'}$C–^{1}C–^{2}C(=O)–^{3}O skeleton.

Published on the web May 28, 2010; doi:10.1246/bcsj.20100002

changes absolutely the value of the packing parameter. Thus, we may assume that conformational transitions of the succinate skeleton play a critical role in variation of the shape and size of the aggregate. Details of the droplet–lamellar transition in the AOT–decane–water system were investigated by Nagao et al.[21] and Seto et al.[22,23] using pressure- and temperature-dependent small-angle neutron scattering and small-angle X-ray scattering methods. However, attempts to explain the detailed behavior at a molecular level are as yet not reported.

The dynamic structure of each hydrocarbon chain of AOT reversed micelles was elucidated by ^{13}C NMR methods (^{13}C NMR spin–lattice relaxation and ^{13}C{^{1}H} nuclear Overhauser effect).[24] ^{1}H NMR studies[25,26] of AOT reversed micelles have been made to discuss qualitatively the rotational isomers about the $^{1'}CH_2$–^{1}CH segment of the succinate skeleton. However, the role of the conformational transitions of the whole succinate skeleton in the aggregation still remains unresolved, in spite of their paramount importance in the factors governing the disorder–order transition.

Recently, we demonstrated that the droplet–lamellar (D–L) transition occurs very slowly at 298 K in the sodium dioleylsulfosuccinate (SDOleS)/decane/water system, depending upon the extent of hydration.[27] This transition has been successfully interpreted at the molecular level, presenting a model in which the conformational change of the SDOleS molecule from an open type to a closed type may induce the D–L transition as the extent of hydration increases. The possibility exists that the conformational change of the succinate skeleton, arising from a change in the extent of hydration, may play an important role in this D–L transition. Thus further detailed study of the conformations for the whole succinate skeleton is highly desirable.

The purpose of the present paper is to apply evidence from the IR spectra of some AOT-homologs, whose crystalline structure has been analyzed by single-crystal X-ray diffraction studies,[28,29] to an investigation of the conformations of the whole succinate skeleton in aqueous solution.

In the present paper, conformations of the whole succinate skeleton in aqueous solution are presented in detail, using evidence based on the IR spectra of some AOT-homologs. The results lead to identification of IR spectroscopy as a powerful tool for elucidation of the mechanism of such a D–L transition.

Experimental

Materials. A series of sodium dialkylsulfosuccinates (sodium 1,2-bis(alkoxycarbonyl)ethanesulfonate) (SDAS) was synthesized as follows. Reactions of maleic acid anhydride with the corresponding alcohol were performed in dried benzene under reflux ($T = 328$ K) for 4 h in the presence of concd H_2SO_4. Dialkyl esters of maleic acid thus obtained were distilled at 3 mmHg (boiling points: 330.2–331.1 K for the dimethyl ester, 342.8–346.2 K for the diethyl ester, 367.4–370.0 K for the dipropyl ester, 380.7–382.7 K for the dibutyl ester), 1.5 mmHg (boiling points: 411.4–412.4 K for the dihexyl ester) and 0.1 mmHg (boiling points: 401.2–420.15 K for the dioctyl ester). Each purified maleic acid ester was sulfonated with an equimolar amount of sodium hydrogensulfite in H_2O at 373 K. Sodium dimethylsulfosuccinate (SDMS), sodium diethylsulfosuccinate (SDES), sodium dipropylsulfosuccinate (SDPS), sodium dibutylsulfosuccinate (SDBS), sodium dihexylsulfosuccinate (SDHS), and sodium dioctylsulfosuccinate (SDOS), thus prepared, were recrystallized in H_2O–methanol. Sodium diheptylsulfosuccinate (SDHpS), sodium didecylsulfosuccinate (SDDS), and sodium didodecylsulfosuccinate (SDDoS) were prepared according to standard procedures.[30,31]

All the reactants for preparation of these SDAS compounds were purchased from Wako Chemicals Co., and were purified before use. The reactants for the preparation of SDHpS, SDDS, and SDDoS were purchased from Aldrich or Avocado Chemicals and were used without further purification. Sodium bis(2-ethylhexyl)sulfosuccinate (Aerosol-OT, AOT) (pure grade) was purchased from Tokyo Kasei Co., Ltd. (Tokyo), and was purified using a published method.[32] The solid AOT sample thus purified was stored in a vacuum desiccator over P_2O_5.

Identification of the samples other than AOT was confirmed from ^{13}C NMR spectra and by elemental analysis (C, H, and S %, the agreement between the calculated and experimental values was within $\pm 0.5\%$).

The amounts of hydrated water for each crystalline SDAS thus synthesized were well-controlled by changing the growth rate of the crystals and were determined by Karl–Fisher titration (Kyoto Electric Co.). For the solid AOT samples, the times for drying in a desiccator over P_2O_5 were controlled. The controlled hydration numbers of SDAS$\cdot n$H$_2$O and AOT$\cdot n$H$_2$O (n = hydration number) were: SDMS$\cdot$1.2H$_2$O, SDES$\cdot n$H$_2$O (n = 1.2, 1.9, and 3.2), SDPS$\cdot$6.2H$_2$O, SDBS$\cdot n$H$_2$O (n = 1.3, 2.4, and 3.4), SDHS$\cdot n$H$_2$O (n = 1.2 and 2.3), SDHpS$\cdot n$H$_2$O (n = 1.2 and 2.2), SDOS$\cdot n$H$_2$O (n = 1.2 and 2.2), SDDS$\cdot$1.1H$_2$O, SDDoS$\cdot$1.5H$_2$O, AOT$\cdot$3.5H$_2$O, and AOT$\cdot$6H$_2$O. For the hygroscopic AOT samples, it is possible that variation of the hydration number will be present during measurement of their infrared absorption spectra. Accordingly, the hydration numbers of these samples were determined from the relative intensities of the infrared absorption bands arising from the C–H stretching modes (2800–3100 cm^{-1}) of the alkyl chains and from the O–H stretching modes (3200–3700 cm^{-1}) of hydrated water.

Methods. Infrared absorption (IR) spectra of the solid samples were recorded on a Nicolet Magna 750 Fourier transform IR spectrometer, operating at a resolution of 2 cm^{-1} at 298 K. For aqueous samples, the solution was sandwiched between two CaF_2 windows with spacers (9–12 mm), and the sample compartment was continuously purged with dried nitrogen during data acquisition. The presented frequencies in this paper are accurate to ± 1 cm^{-1} for sharp bands and 2–3 cm^{-1} for broad bands. X-ray diffraction patterns of the SDHS aqueous solutions were obtained by use of an RAD-RC diffractometer with counter-monochrometer (Cu Lα, 50 kV, 110 mA).

The phase map of the SDHS–H_2O solutions was determined by visual inspection and confirmed by X-ray diffraction methods (map not shown). The sample solutions were prepared by weighing the sample and water into glass ampoules which were sealed and the contents were homogenized by shaking. The phase features of the samples were observed by visual inspection while they were held in a temperature-controlled water-bath. It was confirmed that the aqueous solutions of

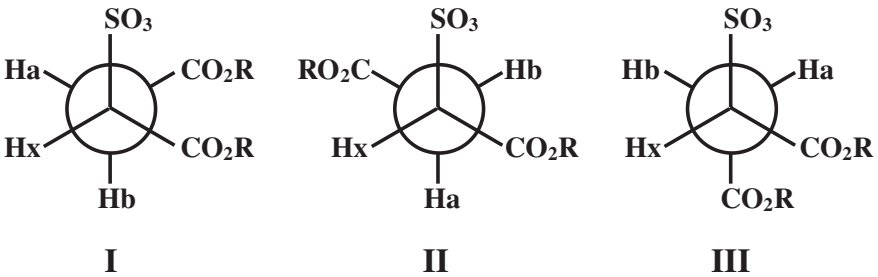

Scheme 2. Rotational isomers **I**, **II**, and **III** possible about the CH_2–CH single bond of the succinate segment.

SDHS below 50 wt % were in an isotropic phase and the samples in the range of 50–75 wt % were in a lamellar phase (spacings of the reflections detected for the aqueous samples above 60 wt % at 298 K were 30.23, 15.99, and 10.04 Å and the lamellar thickness for the aqueous samples above 60 wt % at 298 K was 30.23 Å).

The electrical conductivity method was used to determine the critical micelle concentration (cmc) from a plot of specific electrical conductivity (κ) against the surfactant concentration (C). This plot furnished two straight lines intersecting at the cmc. The electrical conductivities of the sample solutions were measured with a Conductivity Meter CG-2A (TOA Electronics Ltd.) and with a conductivity cell CG-7001PL (cell constant: 0.995×0.1) at 298.15 ± 0.01 K. Ultra-pure water, which had been allowed to stand overnight, in order to prevent the carbon dioxide effect on the conductivity during the measurements, was used as solvent. The value of cmc thus obtained for the SDHS–water binary system is 6.95 wt %. Thus, it has been confirmed that the SDHS aqueous samples of 10–50 wt % used for IR measurements were micellar solutions.

Light-scattering measurements, to determine the molecular weights of the SDHS micelles, were carried out on an Otuka Elecronic SLS-6000 light-scattering photometer using He-Ne laser light (5 mW) at 632.8 nm. The refractive index increment of the sample solutions was measured on an Otuka electronic DRM-1021 differential refractometer at 63.3 nm. Distilled water was used as solvent and each sample solution was filtered through a 0.02 μm membrane, before measurements were taken. The temperature was kept at 298.15 ± 0.01 K by circulating temperature-controlled water through the cell housing. The apparent weight-average molecular weight (M_w) and aggregation number (n) of the SDHS micelles thus obtained were $M_w = 5243$ and $n = 16.5$, respectively.

Results and Discussion

The crystal structure of sodium dimethylsulfosuccinate monohydrate, SDMS·$1H_2O$; sodium diethylsulfosuccinate trihydrate, SDES·$3H_2O$; and sodium diheptylsulfosuccinate dihydrate, $SDH_pS \cdot 2H_2O$; have been analyzed by use of the single-crystal X-ray diffraction method.[28,29] The results indicated that, of the three rotational isomers **I**, **II**, and **III** possible around the $^{1'}CH_2$–^{1}CH single bond of the succinate segment (Schemes 1 and 2), one isomer of type **III** is stabilized in its crystalline state.

In our previous paper,[16] the torsion angles (θ°) of the succinate skeletons (^{2}C–^{1}C–$^{1'}C$–$^{2'}C$, $^{1'}C$–^{1}C–^{2}C–^{3}O, and ^{1}C–$^{1'}C$–$^{2'}C$–$^{3'}O$) (Scheme 1) for the R(*rectus*)-forms of two stereoisomers of SDMS·$1H_2O$, SDES·$3H_2O$, and SDHpS·$2H_2O$ were calculated by the use of X-ray diffraction data.[28,29] The results are summarized as follows. For SDMS·$1H_2O$, SDES·$3H_2O$, and SDHpS·$2H_2O$, the torsion angles of the ^{2}C–^{1}C–$^{1'}C$–$^{2'}C$ skeleton are −60.8, −64.7, and −62.6°, respectively, and those of the ^{1}C–$^{1'}C$–$^{2'}C$–$^{3'}O$ skeleton (α-chain) are −177.0, −168.3, and −167.9°, respectively. From these torsion angles of the α-chain, we find that the succinate skeleton of the three sulfonates is approximately in the extended form. Conversely, the torsion angles of the $^{1'}C$–^{1}C–^{2}C–^{3}O skeleton of the β-chain are 140.4° for SDMS·$1H_2O$ and 141.2° for SDES·$3H_2O$, indicating that the β-chain of SDMS and SDES does not take up both the *trans*- and *gauche*-forms for the conformations about the ^{1}C–^{2}C single bond. In particular, we note that the torsion angle (17.5°) for SDHpS·$2H_2O$ differs markedly from those of SDMS·$1H_2O$ and SDES·$3H_2O$. This fact implies that there exists a marked difference in the configurations of the $^{1'}C$–^{1}C–^{2}C–^{3}O skeleton for the β-chain of SDMS·$1H_2O$ and SDES·$3H_2O$ compared with that of SDHpS·$2H_2O$. We may emphasize that the configuration, $\theta = 17.5$, of SDHpS·$2H_2O$ might be induced by stacking of *n*-heptyl chains in the crystalline state.

Figure 1 shows the two conformations, A and B, possible for a diethylsulfosuccinate anion, arising from such a difference in the torsion angles of the $^{1'}C$–^{1}C–^{2}C–^{3}O segment. For the SDAS anions with longer hydrocarbon chains,[16] the two hydrocarbon chains of type A fan out, while those of type B are aligned approximately parallel to each other. The former type may be referred to as an open-type conformation while the latter type is a closed-type conformation. In particular, type B strongly contributes to a stacking structure between hydrocarbon chains in the crystalline state.[28] Detection of this conformation in the SDAS series leads to elucidation of the contribution of the hydrophobic interactions to the stacking structure.

Thus, the torsion angles of the $^{1'}C$–^{1}C–^{2}C–^{3}O skeleton, in addition to the three rotational isomers around the $^{1'}CH_2$–^{1}CH single bond (Scheme 2), may be regarded as one of factors governing the directionality of the two hydrocarbon chains in an aggregate of SDAS anions.

IR Spectra of the Solid SDAS Series and Conformations of the Succinate Skeleton. The marked difference in the torsion angles of the succinate skeleton between SDES·$3H_2O$ (or SDMS·$1H_2O$) and SDHpS·$2H_2O$ should be reflected in their IR spectra. We have already reported the IR spectra of a series of the crystalline SDAS, in connection with the effect of crystal polymorphism on the environment of the succinate moiety.[15]

In this present study, the IR spectra of the crystalline SDAS series, well-controlled in hydration number, were re-measured to investigate the effect of the different torsion angles.

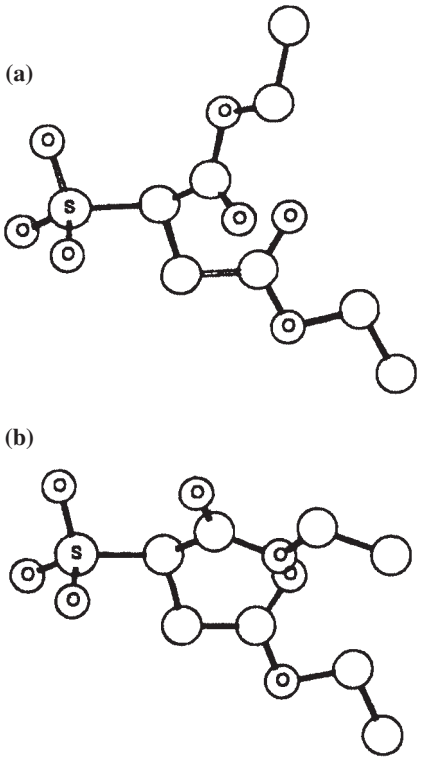

Figure 1. Two conformations (a: type A ($\theta = 141.2°$) and b: type B ($\theta = 17.5°$)) arising from the difference in the torsion angles (θ) of the $^{1'}C$–^{1}C–^{2}C–^{3}O skeleton of a diethylsulfosuccinate anion.

The vibrational spectra of SDAS consist of the vibrational modes arising from all of the two alkyl chains, the succinate segment, and the sulfonate and the two ester portions. We therefore expect that there will be complications in their vibrational spectra in the regions 500–700, 1000–1500, and 1700–1750 cm^{-1}.

In our previous paper,[17] we examined the vibrational spectra of SDMS, SDES, and their deuterated (deuterated dimethyl and deuterated diethyl) compounds. The results provided direct evidence that the region 1300–1430 cm^{-1} reflects CH_2-scissoring, CH-deformation, and their coupled modes for the $^{1'}CH_2$–^{1}CH segment (Scheme 1). The IR bands in this region for a series of SDAS are listed in Table 1 and the IR spectra of crystalline SDHS samples, as representatives, are shown in Figure 2. We discuss below the IR evidence that such a marked difference in the torsion angles is reflected in the vibrational modes of the $^{1'}CH_2$–^{1}CH segment.

It is already known that the wagging modes arising from the CH_2 groups of *n*-alkyl chains also appear at 1365–1370 cm^{-1}.[33] However, in general, IR intensities of these vibrational modes are very weak compared with those of the CH_2-deformation modes (1450–1460 cm^{-1}) of alkyl chains. Accordingly, we may assume that the CH_2- and CH-deformation modes of the succinate segment are predominantly observed in the 1300–1450 cm^{-1} region. In fact, these characteristic bands are commonly observed in the IR spectra of the SDAS series, irrespective of the chain length but dependent upon the hydration number (Table 1, discussed below).

The IR bands of the CH_2- and CH-deformation modes characteristic of the $^{1'}CH_2$–^{1}CH segment for SDMS·1.2H_2O, SDES·3.2H_2O, and SDHpS·2.2H_2O are listed in Table 1. These three samples are not single crystals but the hydration numbers 1.2 for SDMS, 3.2 for SDES, and 2.2 for SDHpS are very close to those for SDMS·1H_2O, SDES·3H_2O, and

Table 1. IR Bands[a] (cm^{-1}) Arising from the CH_2 and CH Deformation Modes Characteristic of the Succinate Segment for a Series of Crystalline SDAS (Non-Single Crystals) and for Solid AOT in the 1300–1430 cm^{-1} Region[b]

	IR band/cm^{-1}					
SDMS·1.2H_2O	1416m		1376m		1348vs	
SDES·1.2H_2O	1422vs	1396s	1374vs		1342vs	
SDES·1.9H_2O	1422vs	1396s	1374vs		1342vs	
SDES·3.2H_2O	1422vs	1396s	1374vs	**1360sh**	1342vs	**1314m**
SDPS·6.2H_2O	1418vs	1398s	1377w	**1357vs**	1337vs	**1316vw**
SDBS·1.3H_2O	1418vs	1398s	1374w	**1358w**	1345vs	**1315vw**
SDBS·2.4H_2O	1418vs	1397s	1374w	**1358m**	1346vs	**1315vw**
SDBS·3.4H_2O	1416vs	1396s	1380w	**1358s**	1345m	**1316vs**
SDHS·1.2H_2O	1418s	1398s	1377sh	**1364m**	1345vs	**1315w**
SDHS·2.3H_2O	1420vs	1402s	1380sh	**1366vs**	1346w	**1316vs**
SDHpS·1.2H_2O	1418vs	1398s	1377sh	**1365m**	1344vs	**1316vw**
SDHpS·2.2H_2O	1420vs	1400s	1380sh	**1365vs**	1346w	**1316vs**
SDOS·1.2H_2O	1418s	1398m	1376m		1345s	
SDOS·2.2H_2O	1420s	1400m		**1366m**		**1316m**
SDDS·1.1H_2O	1418s	1400m		**1366m**		**1316m**
SDDoS·1.5H_2O	1418s	1400m		**1366m**		**1316m**
AOT·3.5H_2O	1416m	1400m	1380m	**1360m**	1344vs	**1313vw**
AOT·6H_2O	1416m	1394m	1382m	**1364m**	1345w	**1314m**

a) vs: very strong, s: strong, m: medium, w: weak, vw: very weak. b) For the single crystals of SDMS·1H_2O, SDES·3H_2O, and SDHpS·2H_2O, crystal structures have been confirmed by X-ray diffraction analysis (Refs. 28 and 29). The bold-faced wavenumbers designate type-B characteristic bands.

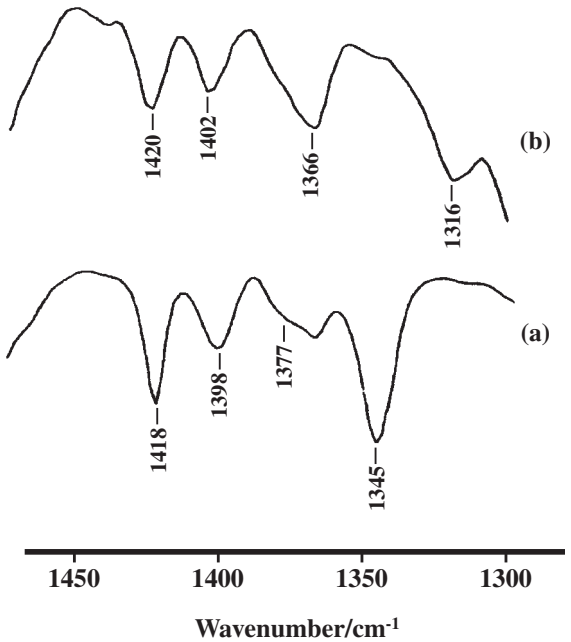

Figure 2. The IR spectra of SDHS·1.2H_2O (a) and SDHS·2.3H_2O (b) in the region 1300–1450 cm^{-1}.

SDHpS·2H_2O, respectively, whose single-crystal structures are known.[28,29] Therefore, it may be assumed that the IR bands of these samples reflect the marked difference in the torsion angles of the $^{1'}C$–^{1}C–^{2}C–^{3}O skeleton between SDES·3H_2O (or SDMS·1H_2O) and SDHpS·2H_2O.

The IR spectra of these SDAS species provide bands in common at 1396–1402 and 1416–1422 cm^{-1}, which are assigned to the CH-deformation mode and the coupled modes between the CH-deformation and the CH_2-scissoring for the succinate segment, respectively.[17] We note that there exists a marked difference in the 1300–1390 cm^{-1} region among the IR spectra of these compounds. The SDES·3.2H_2O sample provides very strong bands at 1342 and 1374 cm^{-1} while SDHpS·2.2H_2O furnishes strong bands at 1316 and 1365 cm^{-1}. We may assume that such a marked difference arises from the difference in the torsion angles of the $^{1'}C$–^{1}C–^{2}C–^{3}O skeleton. Accordingly, the bands at 1342 and 1374 cm^{-1} may be regarded as the bands characteristic of type A conformation while the 1316 and 1365 cm^{-1} bands are those characteristic of type B (Figure 1).

The molecular structures of single crystals of SDES·1.2H_2O and SDES·1.9H_2O have not yet been elucidated by X-ray diffraction analysis. However, since their IR spectra provide strong bands at 1342 and 1374 cm^{-1}, corresponding well to those of SDES·3.2H_2O (Table 1), we may assume that the $^{1'}C$–^{1}C–^{2}C–^{3}O skeleton for the two SDES samples also takes up a torsion angle approximately equal to 141.2°. Thus, the conformation of the succinate skeleton for the SDES samples may be regarded as type A. When the hydration number is greater than three, shoulder bands appear at 1360 and 1314 cm^{-1} with an increase in intensity (spectra not shown), indicating that a further increase in hydration number induces type B conformation.

The IR spectra of the SDPS samples with different hydration numbers were not measured in this study. However, for SDPS·6.2H_2O it was confirmed that the bands at 1337 and 1377 cm^{-1} correspond well to the 1342 and 1374 cm^{-1} bands, respectively, of SDES·3.2H_2O, and those at 1316 and 1357 cm^{-1} to the 1316 and 1365 cm^{-1} bands, respectively, of SDHpS·2.2H_2O (Table 1). Thus, we may assume that types A and B conformations probably coexist in crystalline SDPS·6.2H_2O.

In the IR spectra of the crystalline SDBS samples, we see that the extent of hydration number also affects spectral features in this region (Table 1). In fact, for SDBS·1.3H_2O and SDBS·2.4H_2O, the bands (1374 and 1345–1346 cm^{-1}) characteristic of type A are predominant while for SDBS·3.4H_2O those (1358 and 1315 cm^{-1}) characteristic of type B are intensified.

The IR spectra of SDHS·2.3H_2O and SDOS·2.2H_2O, as well as that of SDHpS·2.2H_2O, provide type B bands (Table 1). The IR bands at 1316 and 1366 cm^{-1} for SDHS·2.3H_2O, as shown in Figure 2b, arise from type B conformation. For SDOS·2.2H_2O, only the bands at 1316 and 1366 cm^{-1} are found and these are assigned to a type B conformation. These observations imply that the $^{1'}C$–^{1}C–^{2}C–^{3}O skeleton of the SDHS and SDOS molecules, as well as that of the SDHpS·2.2H_2O molecule, take up the torsion angles characteristic of type B. In the IR spectra of SDHS·2.3H_2O, bands characteristic of type A are also observed (Table 1). These bands probably arise from coexistence of the monohydrates ($n = 1.2$).

On the other hand, in the IR spectra of the SDHS, SDHpS, and SDOS monohydrates ($n = 1.2$), bands (1344–1345 and 1376–1377 cm^{-1}) characteristic of type A are predominant. Bands (1316 and 1376–1380 cm^{-1}) characteristic of type B, probably coming from the slight coexistence of the dihydrate ($n = 2.2$) samples, are also observed as extremely weak bands or weak shoulder bands (Table 1). These results indicate that the torsion angles of the $^{1'}C$–^{1}C–^{2}C–^{3}O skeleton for these monohydrates may be very near to that for SDES·3.2H_2O.

These observations give clear evidence that the $^{1'}C$–^{1}C–^{2}C–^{3}O skeleton of these SDAS molecules with longer hydrocarbon chains may take up torsion angles of either type A or type B conformations, depending upon the magnitude of the hydration number.

For a series of SDAS with hydrocarbon chains up to and including 8 carbon atoms, an increase in hydration number probably brings about a conformational change for the succinate skeleton from type A to type B. However, for SDAS with longer hydrocarbon chains (for example, SDDS and SDDoS) (Table 1), the type B conformation of the succinate skeleton may be stabilized even in the monohydrated (1.1H_2O) or one and half-hydrated (1.5H_2O) states.

Thus, the longer hydrocarbon chains of SDDS and SDDoS may promote stabilization of type B (closed type), implying that the effect of hydration on the conformation around the torsion angle of the succinate skeleton depends strongly upon the length of the alkyl chain. In other words, in the SDAS anions with short chains, such as SDHS, SDHpS, and SDOS, the conformational change around the torsion angles may be affected easily by variation in the hydration structure around the polar groups, due to alteration in the hydrophobic interactions. However, in the SDAS anions with longer hydrocarbon chains, the increased hydrophobic interactions probably stabilize the type B conformation.

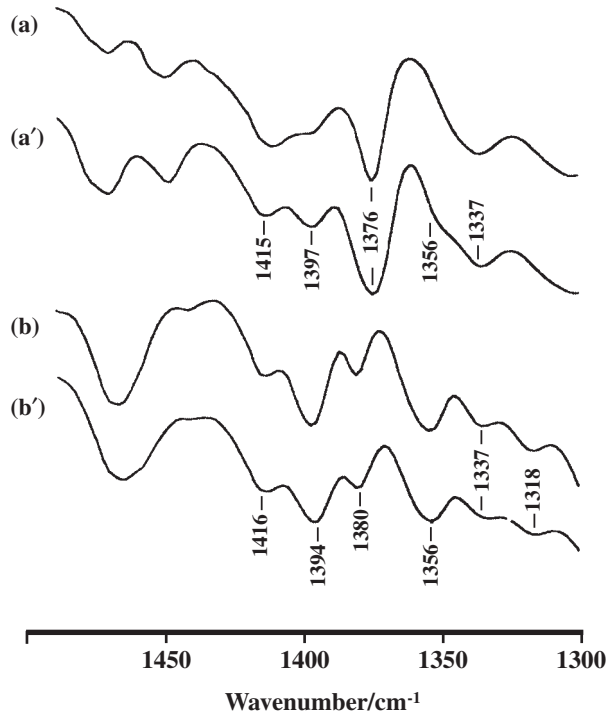

Figure 3. The IR spectra of the aqueous samples of SDES ((a) 20 wt %, (a′) 40 wt %) and SDPS ((b) 20 wt %, (b′) 40 wt %) in the region 1300–1500 cm^{-1}.

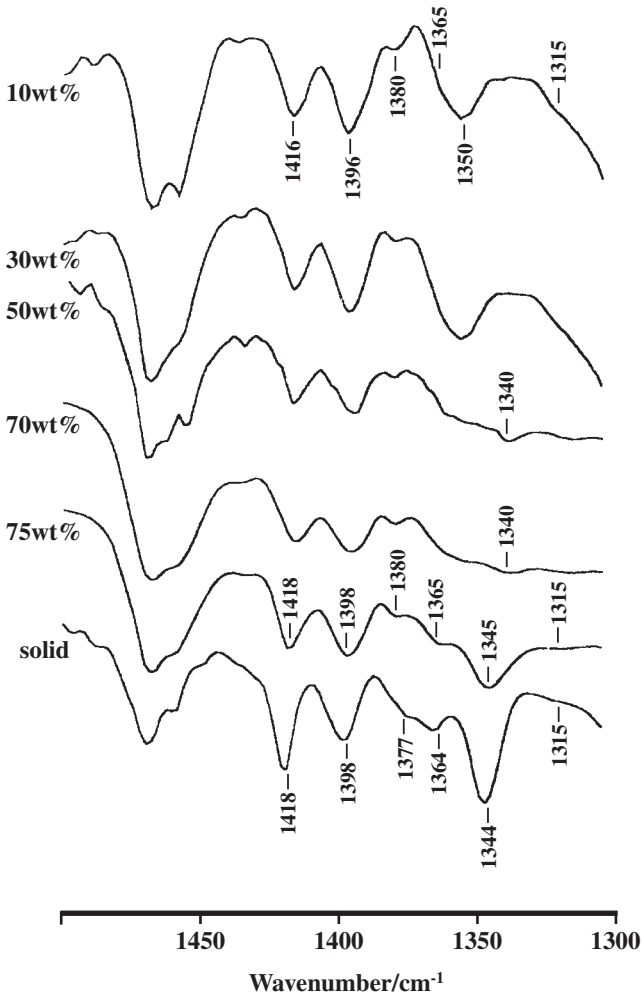

Figure 4. Concentration-dependence of the IR spectrum in the region 1300–1500 cm^{-1} for SDHS aqueous solutions. The IR spectrum of the solid SDHS·1.2H_2O is shown for comparison.

It is likely that the difference in potential minimum between types A and B is very small, as calculated theoretically between the *trans*- and *gauche* (or *gauche*′)-configurations in the internal rotation about a CH_2–CH_2 single bond of butane,[34] although the energy difference has not yet been determined.

For the IR spectra of AOT·6H_2O in the solid state (Figure 5 and Table 1), bands characteristic of the succinate segment are clearly found at 1314, 1345, 1364, 1382, 1394, and 1416 cm^{-1}. The bands at 1345 and 1382 cm^{-1} correspond well to those at 1337–1348 and 1374–1380 cm^{-1}, respectively, characteristic of type A, and the bands at 1314 and 1364 cm^{-1} correspond to the 1314–1316 and 1357–1366 cm^{-1} bands, respectively, characteristic of type B. Since the intensity of the 1345 cm^{-1} band is weaker than that at 1364 cm^{-1}, the type B conformation probably predominates, although types A and B coexist in the solid state.

We may use these IR bands, observed in the crystalline SDAS samples, which are characteristic of types A and B, to discuss the conformations of the succinate skeleton of AOT and its homologs in aqueous solutions.

IR Spectra of the Aqueous SDAS Samples and Conformations of the Succinate Segment. Figure 3 shows the concentration-dependence of the IR spectrum for aqueous solutions of SDES and SDPS in the 1300–1450 cm^{-1} region. For the two aqueous SDES solutions (Figures 3a and 3a′), we see that the IR bands at 1337, 1376, 1397, and 1415 cm^{-1} correspond closely to those at 1342, 1374, 1396, and 1422 cm^{-1}, respectively, characteristic of crystalline SDES·3.2H_2O (Table 1). This observation indicates that the type A conformation of the succinate skeleton in the crystalline SDES is stabilized even in the aqueous samples. The appearance of the shoulder band at 1350–1360 cm^{-1} at a higher concentration (40 wt %) probably implies that an increase in concentration induces type B (closed type).

For aqueous solutions of SDPS (Figures 3b and 3b′), the IR bands at 1318, 1337, 1356, 1380, 1394, and 1416 cm^{-1} correspond closely to the bands at 1316, 1337, 1357, 1377, 1398, and 1418 cm^{-1}, respectively, in the IR spectrum of solid SDPS·6.2H_2O. We may assume that the 1337 and 1380 cm^{-1} bands come from the type A conformer and the 1318 and 1356 cm^{-1} bands from type B. Since the intensity of the 1356 cm^{-1} band is greater than that of the 1337 cm^{-1} band, type B may be preferentially stabilized in both the aqueous samples.

Figure 4 shows the IR spectra in the 1300–1500 cm^{-1} region for the aqueous SDHS samples at various concentrations (10–75 wt %), together with that for the solid SDHS·1.2H_2O. We note that the IR spectrum in the 1300–1450 cm^{-1} region for the concentrated sample (75 wt %) (lamellar solution) is very similar to that for the solid SDHS sample. The bands at 1315, 1345, 1365, 1380, 1398, and 1418 cm^{-1} correspond to the bands at 1315, 1344, 1364, 1377, 1398, and 1418 cm^{-1}, respectively, for the solid SDHS·1.2H_2O. The bands at 1345

and 1380 cm^{-1} for the concentrated samples provide evidence for preferential stabilization of the type A conformer. The existence of the band at 1365 cm^{-1}, in addition to the very weak and broad band at 1315 cm^{-1}, indicates the coexistence of type B. However, since the intensity of the 1345 cm^{-1} band is greater than that of the 1365 cm^{-1} band in the spectrum of the 75 wt % sample (lamellar solution), we may assume that the type A conformation is considerably stabilized compared with the type B conformation, in the concentrated aqueous solution.

For the two diluted samples (10 and 30 wt %) (micellar solutions) (Figure 4), the very broad band at 1350 cm^{-1} could be regarded as the 1345 cm^{-1} band characteristic of type A superimposed upon the band at 1365 cm^{-1} arising from the coexistence of type B. However, we may present an alternative explanation to account for broadening of the 1350 cm^{-1} band. For the micellar solutions (10–50 wt %) of the SDHS solutions, the extent of ordering of the surfactant molecules may be less than that for the lamellar solutions (above 50 wt %). Such an increase in the extent of disorder upon dilution might induce deviation in the torsion angles of the $^{1'}C$–^{1}C–^{2}C–^{3}O skeleton from those of type A or type B. Accordingly, in the dilute solutions, bands different from the 1345 or 1365 cm^{-1} band may appear in this region, causing broadening of the 1350 cm^{-1} band. Thus, we suggest that other conformations, in addition to those of types A and B, may arise from variation of the torsion angles and be present in the isotropic solutions.

Thus, it is evident that for the SDHS solutions, type A conformation of the succinate skeleton is preferentially stabilized in the lamellar solutions, although type B coexists to a great extent, while other conformations, as well those of types A and B, may coexist in the micellar solutions.

The reason that the type A conformation is preferentially stabilized in the SDHS-lamellar solutions may be due to the hydration structure around the succinate moiety arising from the shortness of hydrocarbon chains. The *n*-hexyl chains constituting a SDHS molecule may be too short to provide the stacking structure among the hydrocarbon chains in aqueous solution. In fact, the average aggregation number ($n = 16.5$) of an aqueous SDHS micelle determined by light-scattering method is very small, indicating that the extent of hydrophobic interactions among *n*-hexyl chains is relatively small in the aqueous solution.

The IR spectra of the concentrated AOT solutions (lamellar solutions[35]) are very similar to that of the solid AOT·$6H_2O$, as shown in Figure 5. The bands at 1316, 1340, 1365, 1380, 1396, and 1416 cm^{-1}, observed for the solutions of 50 and 70 wt %, correspond closely to the bands at 1314, 1345, 1364, 1382, 1394, and 1416 cm^{-1}, respectively, for the solid AOT. The band at 1316 cm^{-1} and the shoulder band at 1365 cm^{-1} apparently arise from the type B conformer and the bands at 1340 and 1380 cm^{-1} arise from type A, indicating the coexistence of both types in the lamellar samples. This observation may indicate that, in contrast to the case of SDHS, both type A and type B are stabilized in the concentrated AOT samples. Several factors are likely to contribute to this difference. The presence or absence of branching in the hydrocarbon chains of the constituent molecules is very important in determining the overall molecular steric shape of SDHS and AOT, as is the torsion angle of the succinate skeleton.

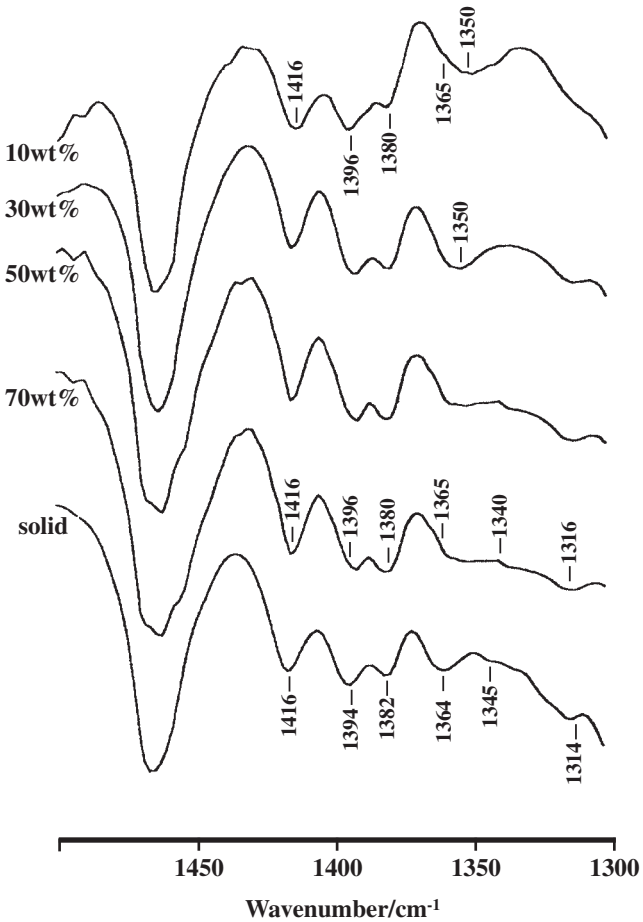

Figure 5. Concentration-dependence of the IR spectrum of AOT aqueous solutions in the region 1300–1500 cm^{-1}. The IR spectrum of solid AOT·$6H_2O$ is shown for comparison.

We note that the IR spectrum in the 1300–1430 cm^{-1} region for the diluted AOT sample (10 wt %) is very similar to that of the diluted SDHS sample (10 wt %). The very broad band at 1350 cm^{-1} for the diluted AOT sample may indicate the presence of the other bands arising from conformations other than types A and B, as discussed above for the diluted SDHS sample.

Thus, for the aqueous samples of the SDAS series and AOT, the IR spectra reflecting the CH_2- and CH-deformation modes of the succinate skeleton can be explained qualitatively using the bands characteristic of types A and B in the crystalline state. These observations may result from the small segmental mobility of the succinate skeleton in the aggregate systems, as discussed below.

Segmental Mobility of the Succinate Skeleton and Its Extremely Restricted State. It is well-known that the steric effect of the bulky $-SO_3^-$ group brings about extreme restriction of the CH_2–CH_2 single bond rotation.[1] For a series of SDAS, we may assume that steric repulsion among the bulky $-SO_3^-$ group and the two carbonyl groups (^{2}CO and $^{2'}CO$) results in stabilization of a specific conformation of the possible isomers of the succinate skeleton. Indeed, in the crystals of SDES·$3H_2O$[29] and SDHpS·$2H_2O$,[28] it has been confirmed that not only does preferential stabilization of the rotational isomer **III** about the ^{1}CH–$^{1'}CH_2$ single bond occur,

but also stabilization of a specific torsion angle for the $^{1'}C$–^{1}C–^{2}C–^{3}O skeleton.[16] The IR spectral data of aqueous solutions for SDES, SDPS, SDHS, and AOT, in this present study, provide clear evidence that this steric effect brings about the restricted state of the succinate skeleton in aqueous solutions.

In our previous paper,[25] we found that, for the reversed micellar system of the AOT–C_6D_6–D_2O (2:2:1), the rotational isomer **III** (Scheme 2) is preferentially stabilized ($P_{\mathbf{I}}$:$P_{\mathbf{II}}$:$P_{\mathbf{III}}$ = 0.21:0.04:0.75; $P_{\mathbf{I}}$, $P_{\mathbf{II}}$, and $P_{\mathbf{III}}$: fractional populations of the rotational isomers **I**, **II**, and **III**, respectively, Scheme 2). This result showed that the $^{1'}CH_2$–^{1}CH group of the succinate segment is extremely restricted in the reversed micelles.

We have no evidence for the values of $P_{\mathbf{I}}$, $P_{\mathbf{II}}$, and $P_{\mathbf{III}}$ for aqueous micellar samples of AOT and its homologs. However, we may expect that such populations will change more in the normal micelles, compared with those in the reversed micelles. The reason for this variation is that the internal rotation of the succinate segment in the aqueous micelles will be restricted, due to an increase in the hydrophobic interactions among the chains which will be much more extensive than those in the reversed micells.[36]

Furthermore, in this present study, for the SDMS–D_2O and SDES–D_2O systems, which are unable to form micelles in aqueous solution, we have calculated the fractional populations of the three rotational isomers ($P_{\mathbf{I}}$, $P_{\mathbf{II}}$, and $P_{\mathbf{III}}$) using ^{1}H NMR coupling constants, according to the method described in Ref. 26. The calculated fractional populations are $P_{\mathbf{I}}$:$P_{\mathbf{II}}$:$P_{\mathbf{III}}$ = 0.2:0.2:0.6 for the D_2O solutions (concentration: 20 wt %) of SDMS and SDES, implying that the rotational isomers **I** (20%) and **II** (20%) coexist although isomer **III** (60%) is stabilized. This result may indicate that isomer **III** is relatively stable even in an unaggregated state, compared with the other two isomers. However, we may assume that the presence of isomers **I** and **II** with such fractional populations ($P_{\mathbf{I}}$ and $P_{\mathbf{II}}$: 0.2) causes deviation of the torsion angles of types A and B in the $^{1'}C$–^{1}C–^{2}C–^{3}O skeleton, resulting in broadening of the 1350 cm^{-1} band of the aqueous samples upon dilution.

For the SDES aqueous solutions (20 and 40 wt %), we find that the intensity of the 1397 cm^{-1} band becomes greater with an increase in concentration (Figures 3a and 3b). This observation may be interpreted by further stabilization of the isomer **III**, as follows. In the normal mode analysis of the SDES anion,[17] the isomers **I**, **II**, and **III** provided calculated values of 1387, 1392, and 1399 cm^{-1}, respectively, for the ^{1}CH-deformation mode (or its mode coupled with the scissoring mode of the $^{1'}CH_2$–group). Accordingly, intensification of the 1397 cm^{-1} band may be explained by invoking an increased fractional population of isomer **III**, providing a calculated value of 1399 cm^{-1}. Furthermore, in the IR spectra of the two SDES aqueous samples, it is evident that an increase in concentration brings about the increased width of the 1376 cm^{-1} band, probably caused by the variation of the fractional populations ($P_{\mathbf{I}}$, $P_{\mathbf{II}}$, and $P_{\mathbf{III}}$).

We may assume that dilution of the samples results in variation of such fractional populations for the cases of AOT and its homologs. This variation may be reflected in the very broad and strong IR bands at 1350 cm^{-1} for the diluted samples and in the very broad spectral feature at 1330–1370 cm^{-1} for the concentrated samples.

Thus, the conformational change between type A and type B conformations in the succinate skeleton, in addition to the variation of fractional populations ($P_{\mathbf{I}}$, $P_{\mathbf{II}}$, and $P_{\mathbf{III}}$) about the $^{1'}CH_2$–^{1}CH single bond, may play a critical role in the disorder–order transition.

Structural Model of the SDHS-Lamellar and the IR Data. We may now discuss a model for the lamellar structure in the SDHS aqueous solutions, in which type A is preferentially stabilized. The type A conformation, with the two hexyl chains fanning out each other (Figure 1a), is apparently not suited to formation of the stacking structure. However, when the hydrocarbon chains of the SDHS molecules, constituting a lamellar, take up a position in which they overlap each other (as in a finger-joint), a lamellar formation of the type A conformation may be possible. In this model, we must assume that the thickness of the lamellar should be smaller than twice the molecular length of SDHS. The thickness of the lamellar structure for the present samples, obtained by the X-ray diffraction method, is approximately 30 Å. This value is clearly smaller than that (35.50 Å) of the bilayer calculated using Tanford's equation[37] ($L_{max} = 1.5 + 1.265n_c$, where L_{max} is the maximum length of hydrocarbon chain and n_c is the number of carbon atoms) and the molecular model of adopted by Sheu et al.[38] This evidence supports our suggestion of a finger-joint model for the lamellar structure in the SDHS aqueous solutions.

The thickness (17.9 Å) of a lamellar structure in the AOT–water binary system has been determined by Mori et al.[35] using the small angle X-ray scattering method. It is clear that this value is smaller than twice (ca. 24 Å) the AOT molecular length. The authors presented a model with bending hydrocarbon chains or a tilted bilayer model, in addition to a finger-joint model, to explain this thickness.

The present IR data provide ample evidence that both types A and B are stabilized in the lamellar of the AOT–water system, indicating that the extent of ordering of molecules in the AOT lamellar is as high as seen in the SDHS lamellar. Moreover, the C^{13} spin–lattice relaxation data[24] provide the following analogy. That is, the segmental mobility of two tertiary CH groups, both their side-CH_2 groups, and two ethyl groups in the 2-ethylhexyl chains, may be extremely restricted in the lamellar, compared with those in the normal and reversed micelles.[24] This great rigidity probably allows the ethyl groups as a branching segment to prevent stacking of the ethylhexyl chains, furnishing the grooves among the AOT molecules. Thereby, the bending portions of 2-ethylhexyl chains may fill the grooves to increase the spatial proximity of inter- and intramolecular 2-ethylhexyl chains, possibly providing the thickness, 17.9 Å, of the AOT lamellar. Thus, we present a mixed model of the AOT lamellar, with contributions from a finger-joint model and a bending-hydrocarbon model.

Conclusion

Two conformations, type A and type B, originating from the difference in the torsion angles of the succinate skeleton ($^{1'}C$–^{1}C–^{2}C–^{3}O), in sodium dialkylsulfosuccinate (SDAS) aggregates, can be detected by the IR spectral method in both aqueous solution and in the crystalline state. We may assume that the conformational change between types A and B in the

succinate skeleton makes an important contribution to the disorder–order transition in the aggregate systems. Thus, the IR bands in the 1300–1450 cm^{-1} region, arising from the CH_2- and CH-deformations and their coupled modes, may be used as a powerful tool for a study of the conformation of the whole succinate skeleton.

References

1 a) H. Okabayashi, M. Okuyama, T. Kitagawa, T. Miyazawa, *Bull. Chem. Soc. Jpn.* **1974**, *47*, 1075. b) H. Okabayashi, M. Okuyama, T. Kitagawa, *Bull. Chem. Soc. Jpn.* **1975**, *48*, 2264.

2 H. Okabayashi, M. Abe, *J. Phys. Chem.* **1980**, *84*, 999.

3 H. Okabayashi, T. Yoshida, T. Ikeda, H. Matuura, T. Kitagawa, *J. Am. Chem. Soc.* **1982**, *104*, 5399.

4 C. A. Boicelli, M. Giomini, A. M. Giuliani, *Appl. Spectrosc.* **1984**, *38*, 537.

5 H. MacDonald, B. Bedwell, E. Gulari, *Langmuir* **1986**, *2*, 704.

6 K. Tsukamoto, K. Ohshima, K. Taga, H. Okabayashi, H. Matuura, *J. Chem. Soc., Faraday Trans. 1* **1987**, *83*, 789.

7 H. Okabayashi, K. Tsukamoto, K. Ohshima, K. Taga, E. Nishio, *J. Chem. Soc., Faraday Trans. 1* **1988**, *84*, 1639.

8 A. D'Aprano, A. Lizzio, V. T. Liveri, F. Aliotta, C. Vasi, P. Migliardo, *J. Phys. Chem.* **1988**, *92*, 4436.

9 T. K. Jain, M. Varshney, A. Maitra, *J. Phys. Chem.* **1989**, *93*, 7409.

10 D. J. Christopher, J. Yarwood, P. S. Belton, B. P. Hills, *J. Colloid Interface Sci.* **1992**, *152*, 465.

11 G. Onori, A. Santucci, *J. Phys. Chem.* **1993**, *97*, 5430.

12 J. Eastoe, G. Fragneto, B. H. Robinson, T. F. Towey, R. K. Heenan, F. J. Leng, *J. Chem. Soc., Faraday Trans.* **1992**, *88*, 461.

13 P. D. Moran, G. A. Bowmaker, R. P. Cooney, J. R. Bartlett, J. L. Woolfrey, *Langmuir* **1995**, *11*, 738.

14 Y. Nagasoe, N. Ichiyanagi, H. Okabayashi, S. Nave, J. Eastoe, C. J. O'Connor, *Colloid Polym. Sci.* **1999**, *277*, 947.

15 Y. Nagasoe, N. Ichiyanagi, H. Okabayashi, S. Nave, J. Eastoe, C. J. O'Connor, *Colloid Polym. Sci.* **1999**, *277*, 1051.

16 Y. Nagasoe, N. Ichiyanagi, H. Okabayashi, S. Nave, J. Eastoe, C. J. O'Connor, *Phys. Chem. Chem. Phys.* **1999**, *1*, 4395.

17 Y. Nagasoe, H. Okabayashi, M. Abe, J. Eastoe, C. J. O'Connor, *Vib. Spectrosc.* **2000**, *23*, 151.

18 H. Okabayashi, K. Ohshima, H. Etori, K. Taga, T. Yoshida, E. Nishio, *J. Phys. Chem.* **1989**, *93*, 6638.

19 H. Okabayashi, K. Taga, T. Yoshida, K. Ohshima, H. Etori, T. Uehara, E. Nishio, *Appl. Spectrosc.* **1991**, *45*, 626.

20 J. N. Israelachvili, in *Intermolecular and Surface Forces Second Edition*, Academic Press, New York, **1992**, p. 369.

21 M. Nagao, H. Seto, T. Takeda, Y. Kawabata, *J. Chem. Phys.* **2001**, *115*, 10036.

22 H. Seto, D. Okuhara, Y. Kawabata, T. Takeda, M. Nagao, J. Suzuki, H. Kamikubo, Y. Amemiya, *J. Chem. Phys.* **2000**, *112*, 10608.

23 H. Seto, M. Nagao, Y. Kawabata, T. Takeda, *J. Chem. Phys.* **2001**, *115*, 9496.

24 a) A. Yoshino, H. Okabayashi, T. Yoshida, K. Kushida, *J. Phys. Chem.* **1996**, *100*, 9592. b) M. Ueno, H. Kishimoto, Y. Kyogoku, *J. Colloid Interface Sci.* **1978**, *63*, 113.

25 A. Yoshino, H. Okabayashi, T. Uchida, T. Ogasawara, T. Yoshida, C. J. O'Connor, *J. Phys. Chem.* **1996**, *100*, 8418.

26 A. Yoshino, N. Sugiyama, H. Okabayashi, K. Taga, T. Yoshida, O. Kamo, *Colloids Surf.* **1992**, *67*, 67.

27 S. K. Ghosh, N. Ichiyanagi, H. Okabayashi, A. Yoshino, T. Takeda, C. J. O'Connor, *Bull. Chem. Soc. Jpn.* **2009**, *82*, 664.

28 J. Lucassen, M. G. B. Drew, *J. Chem. Soc., Faraday Trans. 1* **1987**, *83*, 3093.

29 Y. Nagasoe, N. Hattori, H. Masuda, H. Okabayashi, C. J. O'Connor, *J. Mol. Struct.* **1998**, *449*, 61.

30 J. M. Corkill, J. F. Goodman, T. Walker, *Trans. Faraday Soc.* **1965**, *61*, 589.

31 E. F. Williams, N. T. Woodberry, J. K. Dixon, *J. Colloid Sci.* **1957**, *12*, 452.

32 H. Kunieda, K. Shinoda, *J. Phys. Chem.* **1978**, *82*, 1710.

33 J. H. Schachtschneider, R. G. Snyder, *Spectrochim. Acta* **1963**, *19*, 117.

34 H. Kitano, in *Koubunshi no Kagaku*, ed. by S. Kunugi, **2007**, Chap. 5, p. 136.

35 T. Mori, T. Tada, T. Matsumoto, *Nihon Reoroji Gakkaishi* **1997**, *25*, 223.

36 B. Joensson, B. Lindman, K. Holmberg, B. Kronberg, *Surfactants and Polymers in Aqueous Solution*, **1998**, Chap. 2, p. 46.

37 C. Tanford, *J. Phys. Chem.* **1972**, *76*, 3020.

38 E. Y. Sheu, S. H. Chen, J. S. Huang, *J. Phys. Chem.* **1987**, *91*, 3306.